Article

Rapidly Recoverable Thixotropic Hydrogels from the Racemate of Chiral OFm Monosubstituted Cyclo(Glu-Glu) Derivatives

Lu Wang, Xin Jin, Lin Ye, Ai-ying Zhang, Deon Bezuidenhout, and Zeng-guo Feng

Langmuir, **Just Accepted Manuscript** • DOI: 10.1021/acs.langmuir.7b03527 • Publication Date (Web): 07 Nov 2017

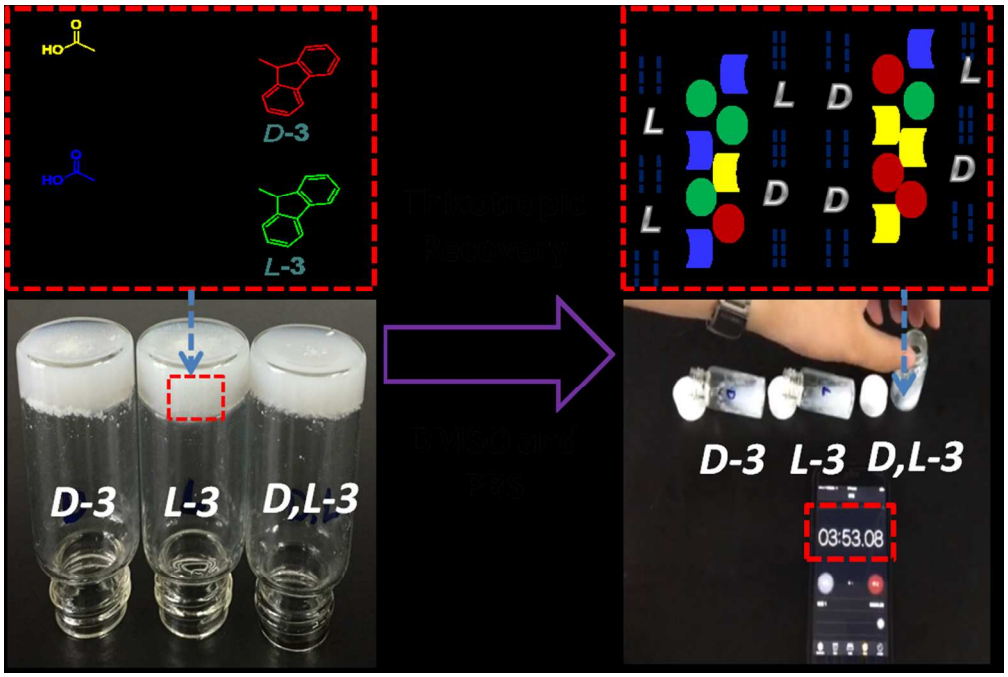

183x122mm (150 x 150 DPI)

Rapidly recoverable thixotropic hydrogels from the racemate of chiral OFm monosubstituted cyclo(Glu-Glu) derivatives

Lu Wang [a], ***Xin Jin*** [a], ***Lin Ye*** [a], ***Ai-ying Zhang*** [a], ***Deon Bezuidenhout*** [b]*, ***Zeng-guo Feng*** [a]*

[a]School of Materials Science and Engineering, Beijing Institute of Technology, No. 5 South Street Zhongguancun, Beijing, 100081

[b]Cardiovascular Research Unit, Chris Barnard Division of Cardiothoracic Surgery, 203 Cape Heart Centre, Faculty of Health Sciences, University of Cape Town, South Africa

ABSTRACT: Both chiral OFm monosubstituted cyclo(*L*-Glu-*L*-Glu) and cyclo(*D*-Glu-*D*-Glu) display a robust gelation ability in a variety of organic solvents and water. In contrast to an individual enantiomer, their racemate can form rapidly recoverable thixotropic hydrogels with a remarkably shorter thixotropic recovery time. This unexpected thixotropic behavior is induced by the random arrangement of *D*- and *L*-enantiomers in the cell units leading to the formation of "pseudoracemate" non-crystalline self-assemblies in the resulting 3D fibrous network.

KEYWORDS: Cyclic dipeptide, racemate, rapidly recoverable thixotropic hydrogel, self-assembly.

INTRODUCTION

Hydrogels fabricated through the self-assemblies of homo- and heterochiral low-molecular-weight gelators (LMWGs) dominated by non-covalent interactions have recently stimulated

considerable interest for their basic research significance and their potential applications in many emerging fields, such as cell culture, drug delivery systems, tissue engineering and regenerative medicine, wound healing and 3D printing due to their flexible shape adaption ability and excellent biocompatibility.[1-12] Among them, 2,5-diketopiperazine (2,5-DKP) or cyclic dipeptide (CDP) derivatives with a rigid six-membered ring containing two chiral centers are revealed to be tailorable and versatile gelator frameworks which not only manipulates the self-assembly process through the hydrogen bonds for one-dimensional arrangement, but also resists enzymatic hydrolysis.[13-19] However, the impact of chirality of gelators on self-assembly behaviours is still amphibolous, despite a large number of studies that have been reported.[20,21] Hence, the elucidation of the functional mechanism of chirality by which influences the construction of organo- and hydrogels remains a great challenge.

To this end, we present a fast tunable thixotropic recovery process of hydrogels created from a racemate (*D,L*-**3**) of cyclo[*L*-Glu(OFm)-*L*-Glu] (*L*-**3**) and cyclo[*D*-Glu(OFm)-*D*-Glu] (*D*-**3**) in a 1:1 molar ratio in this study. To the best of our knowledge, the thixotropic recoverability and persistent recyclability of hydrogels fostered by chiral CDP racemates have seldom been investigated in literature. As the thixotropic recovery time (TRT) is a prerequisite for the structural recoverability of injectable hydrogels after injecting or mechanically stirring for 3D printing and biomedical applications, these TRT tunable thixotropic hydrogels are suitable for the drug controlled release and tissue engineering and regenerative medicine applications

MATERIALS AND METHODS

Materials

H-Pyr-OH was purchased from Han Hong Chemical Technology (Shanghai, China) Ltd. All other reagents (available from Tian Bao Jin Hua Chemical Reagent Company, Beijing, China) were analytical grade and used without further purification unless otherwise noted.

Characterizations

Gelation Tests. A gelator was dissolved into organic solvents or water or a mixture of DMSO and PBS in a 5 mL glass tube with a diameter of 12 mm, and then it was heated to 70 °C to get a clear solution homogeneously and cooled down to room temperature to test whether or not a gel is formed.

Fourier transform infrared spectra. The FTIR spectra of a solution, gel, and solid state were recorded on an IR Trace-100 (Shimadzu) spectrometer. All samples were placed on an IR transparent window and scanned between the wavelengths of 4000 and 400 cm^{-1}.

Transmission electron microscopy. Photos were taken on a JEM 1200EX (JEOL) microscope at 120 kV voltages. The carbon-coated copper grids (300 mesh) were inserted in gel-phase material and dried in vacuum for 2 days.

Field emission scanning electron microscopy. Images were obtained from an S-4800 FE-SEM (Hitachi). The gel samples were prepared by the vacuum freeze-drying method and then coated with gold for 90 s at 5 kV voltages on silicon slices.

Oscillatory rheological testing. The measurements were carried out on a strain-controlled Physica MCR301 rheometer (Anton-Paar) with the parallel plate geometry of diameter 40 mm at 25 °C. The storage and loss modulus were measured with a frequency sweep test (0.1-100 Hz).

^{1}H NMR experiments. All samples prepared in DMSO-d_6 were performed on a Mercury-plus 400 (Varian) at 400 MHz.

Mass spectroscopic measurements. All the mass spectra were recorded on a Xevo G2 QTOF (Waters) high-resolution mass spectrometer.

Elemental analyses. They were performed on a vario EL cube V2.0.1 (Elementar) elemental analyzer.

Melting point tests. They were tested using a DSC-60 instrument (Shimadzu) in a N_2 atmosphere at a heating rate of 10 °C/min.

Wide-angle X-ray diffraction measurements. The WAXS experiments of all the xerogels were monitored by an Ultima IV Instrument (Rigaku) using Cu Kα (λ = 1.5405 Å) radiation with a step size of 0.33 from 3 ° to 60 °.

Synthesis of cyclo(*L*-Glu-*L*-Glu) (*L*-2). Adding 120 ml acetic anhydride and pyridine (v/v=5:1) to a 250 mL round bottom flask, the resulting solution further added with L-pyroglutamic acid (23.22 g, 0.18 mol) was heated to 110 °C until white precipitate appeared and then sustained for 15 mins, stopped, filtered, washed with cold methanol, and dried. The crude product was dissolved in 20 mL concentrated sulfuric acid, and the mixture was slowly added 60 ml distilled water to give rise to white precipitate, stilled for more than 2 hours, filtered, recrystallized in water, and finally dried to get white powder. Yield: 56 %; m.p. = 249 °C; $[\alpha]_D^{20}$ (DMSO, c = 0.1) = -50.03. ^{1}H NMR (400 MHz, DMSO-d_6) δ: 12.13 (s, 2 H, H_e), 8.25 (s, 2 H, H_b), 3.88 (dd, J = 6.62, 5.15 Hz, 2 H, H_a), 2.40-2.23 (m, 4 H, $H_{c,d}$) ppm. IR (KBr) *v*: 3403, 3313, 3196, 3044, 2934, 2864, 2602, 1690, 1400, 1199, 1068, 778 cm^{-1}. TOF-MS: calcd for $C_{10}H_{14}N_2O_6$, 258.08; found,

257.07 ([M-H$^+$]). Elemental analysis: calcd for $C_{10}H_{14}N_2O_6$, C, 46.50; H, 5.48; N, 10.85; found C, 46.32; H, 5.52; N, 10.83.

Synthesis of cyclo[*L*-Glu(OFm)-*L*-Glu] (*L*-3). Briefly *L*-**2** (0.774 g, 3 mmol) was dissolved in 20 mL DMF and the resulting solution was added DIEA (1 mL, 6.1 mmol), Fmoc-Cl (0.779 g, 3.1 mmol) and DMAP (0.036 g, 0.3 mmol) and then sustained for 12 hours at room temperature. Eventually it was filtered, added with water, extracted with ether and supplied with sodium chloride until the aqueous solution was saturated, and then filtered to give rise to white product. Yield: 56.7 %; m.p. = 161 °C; $[\alpha]_D^{20}$ (DMSO, c = 0.1) = -69.0. ^{1}H NMR (400 MHz, DMSO-d_6) δ: 12.05 (s, 1 H, H_k), 8.25(s, 2 H, H_b), 7.90 (d, *J* = 7.5Hz, 2 H, Ph-H_h), 7.64 (dd, *J* = 19.2, 7.3 Hz, 2 H, Ph-H_e), 7.47-7.37 (m, 2 H, Ph-H_g), 7.34 (t, *J* = 7.4Hz, 2 H, Ph-H_f), 3.98-3.71 (m, 2 H, H_a), 2.41-2.12 (m, 4 H, H_d), 1.92 (d, *J* = 6.4 Hz, 4 H, H_c) ppm. IR (KBr) *v*: 3458, 3205, 2964, 1730, 1667, 1449, 1397, 1328, 1254, 1191, 737 cm^{-1}. TOF-MS: calcd for $C_{24}H_{24}N_2O_6$, 436.20, found, 475.49 ([M+K$^+$]); Anal. calcd for $C_{24}H_{24}N_2O_6$: C, 66.04; H, 5.54; N, 6.42; found C, 66.23; H, 5.49; N, 6.48.

Syntheses of cyclo(*D*-Glu-*D*-Glu) (*D*-2) and cyclo[*D*-Glu(OFm)-*D*-Glu] (*D*-3). The synthetic routes of *D*-**2** and *D*-**3** are same with *L*-**2** and *L*-**3**.

RESULTS AND DISCUSSION

Synthesis. Synthetic routes of cyclo(Glu-Glu) *D*- and *L*-enantiomers are illustrated in Scheme 1. According to the literature,[22] *L*- and *D*-pyroglutamic acid were first heated to 110 °C to undertake a dimerization and ring-opening reaction to give rise to glutamic CDPs in the presence of acetic anhydride/pyridine and H_2SO_4/H_2O, and afterwards the acquired cyclo(Glu-Glu)s

underwent esterification reaction with Fmoc-Cl in the presence of DMAP/DIEA.[23] All the compounds were characterized in detail by ^{1}H NMR, MS, IR and elemental analyses (ESI).

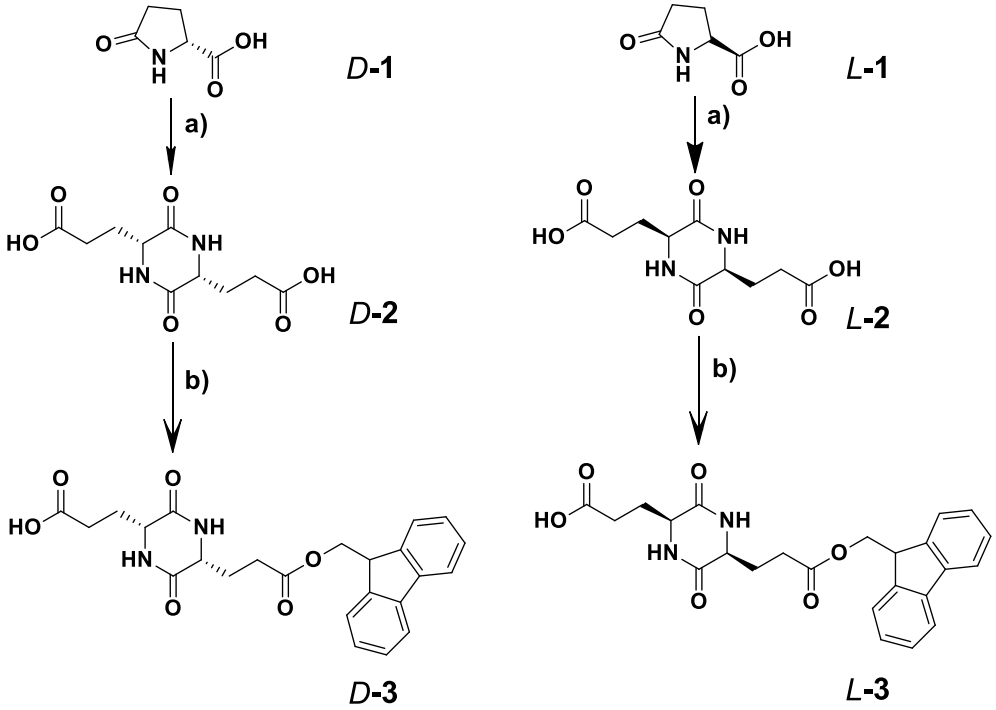

Scheme 1 Synthetic routes of cyclo[*D*-Glu(OFm)-*D*-Glu] (left) and cyclo[*L*-Glu(OFm)-*L*-Glu] (right). a) Acetic anhydride/pyridine/H_2SO_4/H_2O; b) Fmoc-Cl/DMAP/DIEA.

Thixotropic recoverable behaviours of hydrogels. In addition to acting as robust and versatile organogelators toward a variety of organic solvents, both *L*-**3** and *D*-**3** give rise to hydrogels as superhydrogelators at the same, but very low minimum gelator concentration (MGC) of 0.4 wt%, whereas *D,L*-**3** can also form hydrogels at a relatively higher MGC of 0.6 wt% as determined by the tube inversion method in water. However, the hydrogels constructed from the racemate *D,L*-**3** in water, PBS and a 1:5 (v/v) mixture of DMSO and PBS can quickly recover their 3D shape after strongly mechanical stirring compared to its individual enantiomers[24-27]. The TRT values of these hydrogels as a function of concentration of gelators and volume ratio of mixing solvents are summarized in Table 1 and Table S1. As can be seen, at a gelator concentration (GC) of 0.6

wt%, which is slight higher than their MGC, both *L*-**3** and *D*-**3** possess a very long TRT of about 360 mins, whereas *D,L*-**3** gives a significantly short TRT of around 10 mins. When a GC rises to 1.2 wt% (Fig. 1), a TRT of 4 mins for *D,L*-**3** is still substantially shorter than that of 67 mins for *L*-**3** and *D*-**3**. Only when a GC progresses to 1.8 wt%, both the enantiomers and their racemate begin to attain the same TRT level. At the same time, the organogels obtained from *L*-**3**, *D*-**3** and *D,L*-**3** are also thixotropic. As opposed to the hydrogels, there is nearly no difference in the TRT data observed in those organogels just as illustrated in a gel formed in n-hexanol (Fig. S1). Considering the influence of the concentration of a hydrogelator on the compatibility of a hydrogel, the unusual TRT range of 4 to 10 mins at a range of GC of 0.6 to 1.2 wt% for the hydrogels created from the racemate of fluorenemethoxy (OFm) monosubstituted cyclo(Glu-Glu) exhibits the great potential to be used as injectable carriers for drug controlled release and scaffolds for tissue engineering and regenerative medicine.[28-34]

Table 1 TRT data of hydrogels formed from chiral cyclo[Glu(OFm)-Glu] enantiomers in a 1:5 (v/v) mixture of DMSO and PBS.

MGC, wt%	Thixtropic recovery time (mins)		
	D-**3**	*L*-**3**	*D,L*-**3**
0.6	360	360	10
1.2	67	67	4
1.8	2	2	2

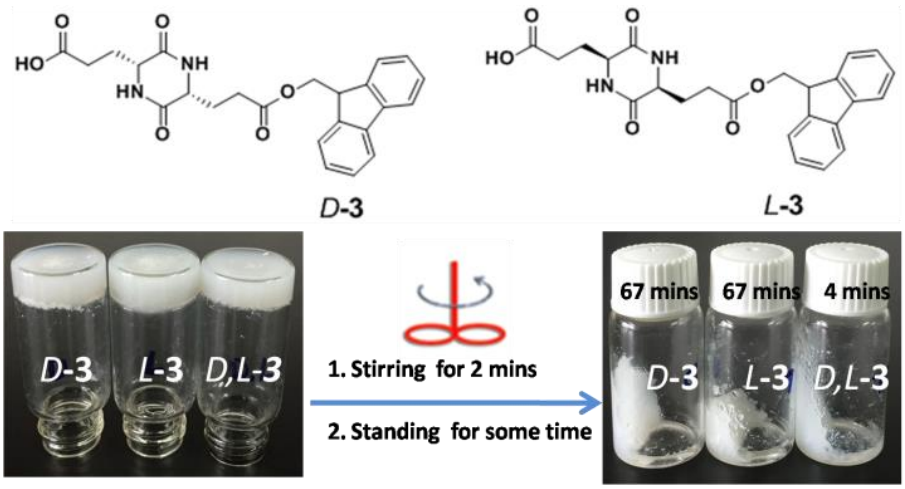

Fig. 1 Thixotropic behaviours of hydrogels formed from *D*-**3**, *L*-**3** and *D,L*-**3** at 1.2 wt% in a 1:5 (v/v) mixing solvent of DMSO and PBS.

Gelation properties and aggregation morphology studies. The ability of the resulting cyclo(Glu-Glu) enantiomers to gel organic solvents and water or PBS was eventually determined by inverting the vials upside down. The gelation testing results and the minimum gelation concentration (MGC, mg/ml) data are summarized in Table 2.

As well known, an optimized balance of hydrophilicity to lipophilicity within the molecular structure is the prerequisite for designing and synthesizing a LMWG to gelate organic solvents and water. However, it remains a great challenge to acurately predict whether or not a molecule is a LMWG. As shown in Table 2, the resulting chiral *D*-**3** and *L*-**3** present the same gelation abilities in a wide range of polar and apolar solvents, whereas the racemic gelator *D,L*-**3** is sparsely soluble in dichloromethane and benzene (Fig. S2). The different gelation ability and MGC values between *D*-**3** or *L*-**3** and *D,L*-**3** hints that the racemate most likely possesses a different self-assembly structure in the 3D fibrous network or crystalline structure in the cell units.

Table 2 Testing results of gelation behaviours and minimum gelator concentration (MGC, wt%) of cyclo[Glu(OFm)-Glu] derivatives by the tube inversion method at room temperature[a,b].

Solvent/sample	*D*-**3**	*L*-**3**	*D,L*-**3**
DMSO	S	S	S
DMF	S	S	S
acetone	S	S	S
dichloromethane	OG(1.0)	OG(1.0)	I
chloroform	TG(1.0)	TG(1.0)	OG(1.5)
hexane	I	I	I
1,2-dichloroethane	TG(0.5)	TG(0.5)	TG(0.5)
tetrachloroethane	TG(0.5)	TG(0.5)	TG(0.5)
MeOH	OG(3.5)	OG(3.5)	S
EtOH	OG(3.0)	OG(3.0)	OG(3.0)
isopropanol	OG(3.0)	OG(3.0)	OG(3.0)
n-butanol	OG(2.5)	OG(2.5)	OG(2.0)
n-hexanol	OG(2.5)	OG(2.5)	OG(2.0)
ethyl acetate	OG(1.5)	OG(1.5)	OG(1.5)
benzene	TG(0.5)	TG(0.5)	I
toluene	TG(0.5)	TG(0.5)	TG(0.5)
o-dichorobenzene	TG(0.5)	TG(0.5)	TG(0.5)
H_2O	OG(0.4)	OG(0.4)	OG(0.6)
PBS	OG(0.4)	OG(0.4)	OG(0.6)

a. *D,L*-**3**, precipitated from a 1:1 molar radio of *D*-**3** and *L*-**3** in water; *b*. TG: translucent gel; OG: opaque gel; S: soluble (>5 wt%); I: insoluble upon heating.

Depending on their chirality, the self-assembled structures of these chiral CDP gelators in organic solvents display intriguing and diverse morphologies such as nematosphere, arborization, fallen hair, grass cluster and cabbage as seen in n-butanol and n-hexonol (Fig. S3). However, as shown by TEM and SEM in Fig. 2, the self-assemblies of the enantiomers *L*-**3** and *D*-**3** in water are featured by uniformly dense tangly fibers, while those of the racemate *D,L*-**3** are characteristic of relatively loose clumped fibers with a relatively larger width in the hydrogels. It appears that these morphological changes do not impact the sol-gel transition temperatures of hydrogels formed from the enantiomers and their racemate (Fig. S4).

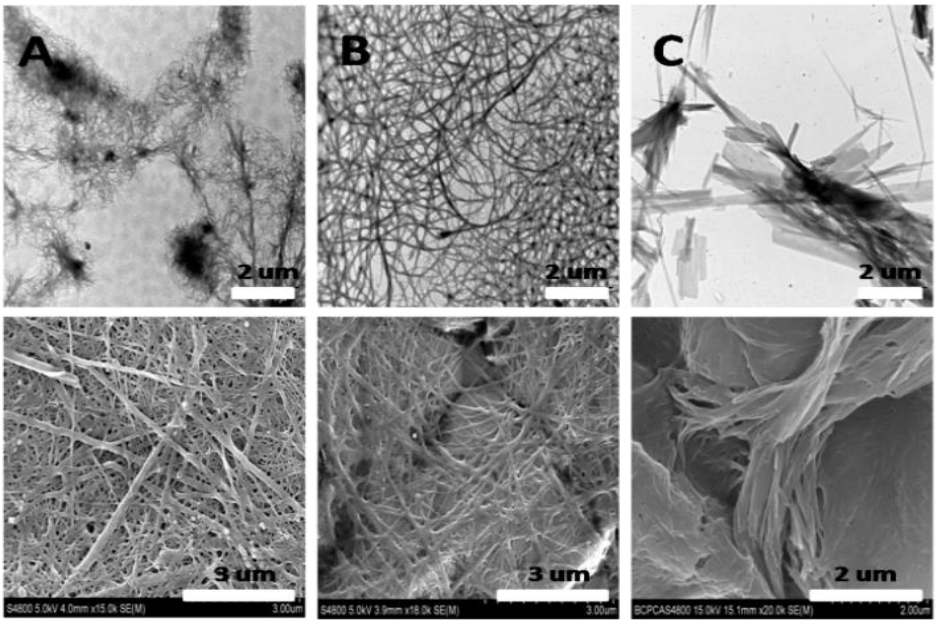

Fig. 2 TEM (upper) and SEM (bottom) morphological images of self-assemblies of of *D*-**3** (A), *L*-**3** (B) and *D,L*-**3** (C) in hydrogels formed in water from left to right.

Rheological measurements. Besides a fast shape recovery, such a thixotropic recoverable hydrogel can also quickly restore its mechanical properties after stirring. To test the mechanical recoverability of the hydrogels formed from *L*-**3** and *D,L*-**3**, dynamic rheological experiments were conducted. The shear strain of 0.1% in the linear viscoelastic region was chosen so that the

G' and G'' would remain constant within the scope of deformation because out of this range, the G' begins to decrease (Fig. S5). Both the G' and G'' for the more highly concentrated hydrogels are evidently larger than that of less concentrated ones, indicating the strength of the hydrogels dependent of the concentration of chiral CDP hydrogelators in this study. For example, the G' of the hydrogel created from *L*-**3** at 1.8 wt% (around 1970 Pa) at 10 Hz is higher than that at 1.2 and 0.6 wt% (approximately 1061 and 871 Pa, respectively), and so is that of *D,L*-**3** at the same concentrations.

Furthermore, the thixotropic recyclability of hydrogels were also elucidated by dynamic rheological measurements. The original hydrogel generated from *L*-**3** is stirred into a sol state. As shown in Fig. 3, when this sol is stood for 67 minutes, the first reformed gel is tested and its G' can achieve 948 Pa at 10 Hz, slightly lower than the original G' of 1014 Pa. Moreover, when this repaired hydrogel is continually stirred and reset for second and third time, the re-evaluated G' and G'' approximate range of original moduli. Significantly, this self-restoring process can be also repeated many times for the racematic hydrogels formed from *D,L*-**3**. For example, its original G' is 1765 Pa at 10 Hz, the first repaired G' attains 1586 Pa after standing for 4 mins, the following repaired ones nearly approach the same G' and G'' values as the original and first repaired ones. Interestingly, the real tested G' and G'' of *D,L*-**3** is distinctly larger than that of *L*-**3** in a whole testing frequency range. This result clearly suggests the potential applications of hydrogels created from *D,L*-**3** as injectable carriers for drug controlled release and scaffolds for tissue engineering and regenerative medicine.[35]

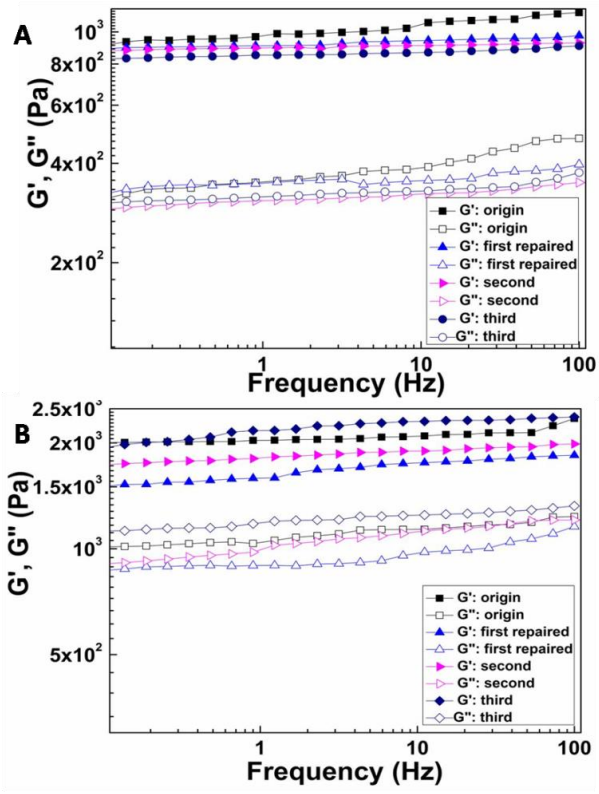

Fig. 3 Rheological data for frequency sweep of original gel and gel after three cycles of *L*-**3** (A) and *D,L*-**3** (B) obtained at 1.2 wt% and at 25 ℃ in a 1:5 (v/v) mixing solvent of DMSO and PBS.

Mechanism of fast thixotropic recoverable behavior. FT-IR and fluorescence spectroscopic analyses were further used to gain insight into the driving forces why and how to present so short and tunable a TRT of the racemic hydrogel of *D,L*-**3** compared to the chiral hydrogels of *D*-**3** and *L*-**3**.[36-40] As can be seen in Fig. S6-8, although a clear difference in characteristic vibration bands between the hydrogel or reformed one of *L*-**3** or *D,L*-**3** and its sheared sol was observed, there is no distinct difference noted between the hydrogel and reformed one of *L*-**3** or *D,L*-**3**. In fact, the gelation behaviors of the racemic gels are a long standing research topic,[41] and these racemic gelators can crystallize into a solid form with different components.[5] In general there are approximately 5-10 % chiral organic compounds giving rise to separate crystals from the opposite isomers in the solution of their racemic mixture. Most of *D*- and *L*-enantiomers are

prone to crystallize to form a racemic crystal referred to as "true racemate" in which the enantiomers are arranged orderly in the cell units. Also there is the third so-called "pseudo-racemate" crystallization process for the racemates, where *D*- and *L*-enantiomers are randomly arranged in the cell units.[42] The gelation is a highly controlled crystallization process where the crystal growth of the gelators almost occur along one dimension so as to form a 3D fibrous network to gelate a large amount of solvent molecules.[3] However, the mechanism by which a racemic aggregate of enantiomer gelators crystallizes or arranges in the cell units remains an unexplored topic. For the as-prepared chiral CDPs here, although both *D*-**3** and *L*-**3** marginally out perform *D,L*-**3** in their gelation capacity, the TRT of the racemate is significantly shorter than that of its individual enantiomers. To highlight the molecular arrangements and orientations of racemate gelator molecules in the hydrogels, the xerogels obtained from the hydrogels of enantiomers *D*-**3** and *L*-**3** and racemate *D,L*-**3** in a 1:5 (v/v) mixing solvent of DMSO and H_2O were measured by WXRD analysis. From the XRD patterns as shown in Fig. 4, nearly the same arrangement structures of self-assemblies are presented by the enantiomers. A possible molecular packing model arranged in the monoclinic P2 group was proposed for their arrangements. Their cell parameters based on the observed XRD pattern by using Jade 6.0 were calculated as follows: a = 8.98 Å, b = 9.82 Å, c = 14.93 Å, β = 103.32 °. Subsequently, the best fitting structure was refined via Reitveld refinement with energy by using Reflex plus module in Materials Studio. Furthermore, these xerogels give rise to a regular second-order diffraction with a *d*-spacing ratio of 1:1/2 (9.67 and 4.94 Å), indicating a lamellar structure.[44]

Intriguingly, it was noted that both *D*-**3** and *L*-**3** are inclined to crystallize in the hydrogels while *D,L*-**3** is prone to self-assemble to an amorphous state in the hydrogels and organogel formed at 8 wt% in CH_3OH as outlined in Fig. S9. This result is consistent with DSC

measurements of xerogels shown in the Fig. S10, revealing that the melting points of *D*-**3** and *L*-**3** are 160 °C and 161 °C with an obvious endothermic peak, while the DSC profile of racemate *D,L*-**3** displays a larger dispersive endothermic peak. It clearly indicates that the racemates in the racematic hydrogels are existed as the "pseudoracemate" non-crystalline self-assemblies in which the two chiral enantiomers are randomly arranged to create the amorphous structure. Intuitively, regular arrangements result in the formation of inside lattice planes so that they are uneasily deformed and need long time to restore original construction after the external force is exerted along the parallel face, while non-crystalline self-assemblies substantially consisting of random molecular arrangements do not need a long time for shape recovery. Hence for the gelation proceeding in this study, the phenomenon we observed that the TRT of the racemic hyrogel is distinctly shorter than its enantiomer counterparts, is most likely boosted by the random arangements of the racemates in the cell units in the hydrogel state. Upon stirring or breaking the hydrogels of *D*-**3** or *L*-**3** and *D,L*-**3**, it is reasoned that the external force destroys inside crystal face structure, and the sol of *D*-**3** or *L*-**3** takes a longer time to self-assemble into the 3D fibrous network for recovering their shapes and mechanical properties. In addition, a much higher enantiomer or racemate concentration enables to narrow the gap of TRTs. As a result, a proposed arrangement model of enantiomers in the hydrogel state is outlined in Fig. S11. For the gelator *D*-**3** or *L*-**3** in a cell unit outlined in green lines, a lamellar organization with a *d* spacing of 9.67 Å was noted. This value is smaller than twice that of the extended molecular length of chiral molecules, but larger than the length of one molecule (about 14.7 Å) calculated by Chemdraw 3D. It suggests that the hydrogel is likely to possess an interdigitated bilayer structure as shown in grey lines, displaying a typical face-to-face manner with outside DKP rings affording N−H···O in rows, inner π−π stacking of fluorenyl rings and COOH. However, in the

"true racemates", the *D*- and *L*-enantiomers are regularly laid out in the cell units as depicted in purple lines in Fig. S12, whereas the "pseudoracemates" illustrate that the molecules of non-crystalline self-assemblies arrange randomly as exhibited in yellow lines in Fig. 5.

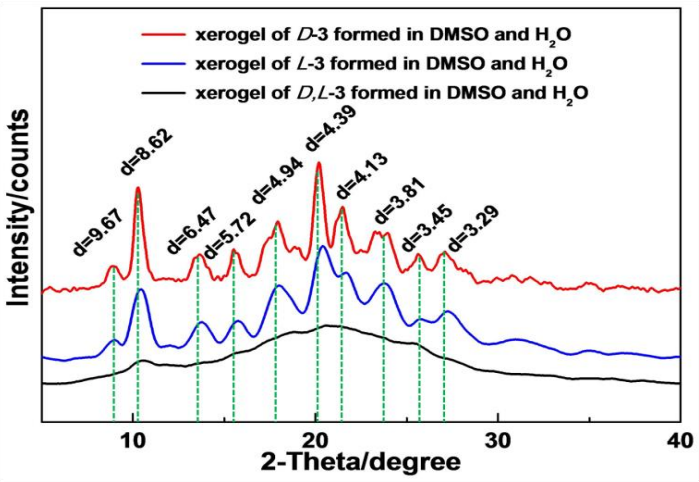

Fig. 4 XRD patterns of xerogels of *D*-**3**, *L*-**3**, and the racemate *D,L*-**3**.

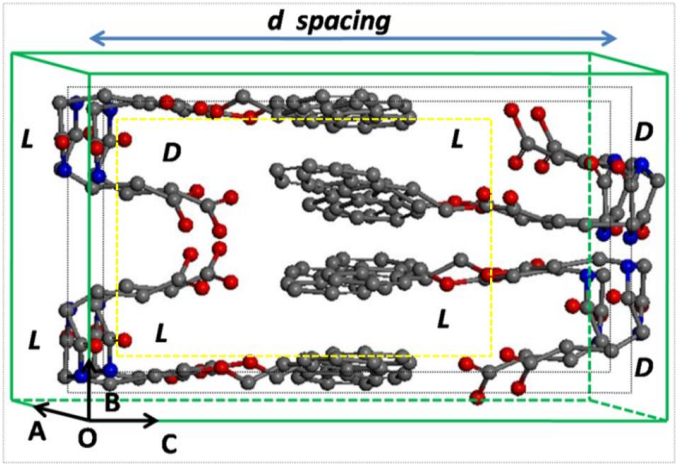

Fig. 5 Proposed molecular arrangement of of hydrogels of the "pseudoracemates" consisting of *D*-**3** and *L*-**3** in cell units.

Conclusion

We synthesized chiral OFm monosubstituted cyclo(Glu-Glu) enantiomers. Their racemate not only enables gelation in a large variety of organic solvents and water, but also displays a fast thixtropic recoverable and recyclable behaviors of hydrogels in H_2O, PBS and a mixture of DMSO and PBS or H_2O. The XRD and DSC analyses indicate that the random arrangements of *D*- and *L*-enantiomers in the cell units contribute to the formation of "pseudoracemate" non-crystalline self-assemblies in the 3D fibrous hydrogel network leading to the rapid thixotropic recoverability and persistent recyclability. The tunable thixotropic recovery time range of 4 to 10 mins at a range of MGC of 0.6 to 1.2 wt% makes the racemate hydrogels potential injectable carriers for the drug controlled release and scaffolds for tissue engineering and regenerative medicine applications.

ASSOCIATED CONTENT

Supporting Information. This material is available free of charge via the Internet at http://pubs.acs.org.

Table S1: Testing parameters of gelation behaviors of cyclo[Glu(OFm)-Glu] derivatives at varying GC and volume ratio of DMSO and PBS.

Figure S1: Thixotropic behaviors of *D*-**3**, *L*-**3** and *D*, *L*-**3** in n-hexanol.

Figure S2: Gel morphologies of *D*-**3** and *D,L*-**3.**

Figure S3: TEM (left) and SEM (right) images of organogels.

Fig. S4: Plot of $T_{sol\text{-}gel}$ as a function of concentration of *D*-**3**, *L*-**3** and *D,L*-**3** under the assist of ultrasound *via* the tube inversion method.

Figure S5: Frequency sweep for the gel of *L*-**3** and *D,L*-**3** at 0.6, 1.2 and 1.8 wt% in a 1:5 (v/v) mixture of DMSO and PBS at 25 °C and at a strain of 0.1 %.

Figure S6: FTIR spectra of hydrogels formed from *L*-**3** (A) and *D,L*-**3** (B) at 25 °C: a: solution in DMSO; b: gel in a 1:5 (v/v) mixture of DMSO and PBS; c: sheared sol; d: reformed gel standing for 12 h.

Figure S7: FTIR spectra of *L*-**3** and *D,L*-**3** in the solid state.

FigureS8: Fluorescence emission spectra of gelator *L*-**3** (A) ($\lambda_{excitation}$ = 290 nm) and *D,L*-**3** (B) ($\lambda_{excitation}$ = 290 nm) in a 1:5 (v/v) mixture of DMSO and PBS at 25 °C.

Fig. S9: XRD patterns of xerogel of *D,L*-**3** formed in CH_3OH and in a 1:5 (v/v) mixing solvent of DMSO and H_2O.

Fig. S10: DSC profiles of *D*-**3**, *L*-**3** and *D,L*-**3** precipitated from a 1:5 (v/v) mixing solvent of DMSO and H_2O.

Fig. S11: Proposed molecular arrangements of hydrogels of *D*-**3** or *L*-**3** in the cell units.

Fig. S12: Proposed molecular arrangements of hydrogels of the “true racemates” in the cell units.

AUTHOR INFORMATION

Corresponding Author

*E-mail: sainfeng@bit.edu.cn; deon.bezuidenhout@uct.ac.za.

Author Contributions

The manuscript was written through contributions of all authors. All authors have given approval to the final version of the manuscript.

Funding Sources

This work was financially supported by the National Natural Science Foundation of China (No. 21174018).

REFERENCES

(1) Liu, G. F., Zhang, D. and Feng, C. L.; Control of three-dimensional cell adhesion by the chirality of nanofibers in hydrogels. Angew. Chem. In. Ed., **2014**, 53, 7789-7793.

(2) Frkanec, L. and Zinic, M.; Chiral bis(amino acid)- and bis(amino alcohol)oxalamide gelators. Gelation properties, self-assembly motifs and chirality effects. Chem. Commun., **2010**, 46, 522-537.

(3) Kim, J. U., Schollmeyer, D., Brehmer, M. and Zentel,R.; Simple chiral urea gelators, (*R*)- and (S)-2-heptylurea: their gelling ability enhanced by chirality. J. Colloid Interf. Sci., **2011**, 357, 428-433.

(4) Taraban, M. B., Feng, Y., Hammouda, B., Hyland, L. L. and Yu, Y. B.; Chirality-mediated mechanical and structural properties of oligopeptide hydrogels. Chem. Mater., **2012**, 24, 2299-2310.

(5) Vujicic, N. S., Glasovac,Z., Zweep, N., van Esch, J. H., Vinkovic,M., Popovic, J. and Zinic, M.; Chiral hexa- and nonamethylene-bridged bis(L-Leu-oxalamide) gelators: the first oxalamide gels containing aggregates with a chiral morphology. Chemistry, **2013**, 19, 8558-8572.

(6) Smith, D. K.; Lost in translation? Chirality effects in the self-assembly of nanostructured gel-phase materials.Chem. Soc. Rev., **2009**, 38, 684-694.

(7) Shen, Z. C., Wang, T. Y. and Liu,M. H.;Tuning the gelation ability of racemic mixture by melamine: enhanced mechanical rigidity and tunable nanoscale chirality. Langmuir, **2014**, 30,

10772-10778.

(8) Friggeri, A., Van Der Pol, C., Van Bommel, K. J., Heeres, A., Stuart, M. C., Feringa, B. L. and van Esch, J. H., Cyclohexane-based low molecular weight hydrogelators: A chirality investigation. Chemistry, **2005**, 11, 5353-5361.

(9) Tomatsu, I., Peng, K. and Kros, A.; Photoresponsive hydrogels for biomedical applications. Adv. Drug Deliver. Rev., **2011**, 63, 1257-1266.

(10) Wang, H., Yang, C., Tan, M., Wang, L., Kong D. and Yang, Z., A structure-gelation ability study in a short peptide-based 'Super Hydrogelato' system. Soft Matter, **2011**, 7, 3897-3905.

(11) Shao, H. and Parquette, J. R.; A pi-conjugated hydrogel based on an Fmoc-dipeptide naphthalene diimide semiconductor. Chem. Commun., **2010**, 46, 4285-4287.

(12) Misra, R., Sharma, A., Shirs, A. and Gopi, H.; Backbone engineered γ-peptide amphitropic gels for immobilization of semiconductor quantum dots and 2D cell culture. Langmuir, **2017**, 31, 7762-7768.

(13) Borthwick, A. D.; 2,5-Diketopiperazines: synthesis, reactions, medicinal chemistry, and bioactive natural products. Chem. Rev., **2012**, 112, 3641-3716.

(14) Geng, H. M., Ye, L., Zhang, A. Y., Li, J. B. and Feng, Z. G.; Low-molecular-weight organo- and hydrogelators based on cyclo(*l*-Lys-*l*-Glu). Langmuir, **2016**, 32, 4586-4594.

(15) Xie, Z. G., Zhang, A. Y., Ye, L., Wang, X. and Feng, Z. G.; Shear-assisted hydrogels based on self-assembly of cyclic dipeptide derivatives. J. Mater. Chem., **2009**, 19, 6100-6102.

(16) Zong, Q. Y., Geng, H. M., Ye, L., Zhang, A. Y., Shao, Z. Q. and Feng, Z. G.; Gelation capability of cysteine-modified cyclo(*L*-Lys-*L*-Lys)s dominated by Fmoc and Trt protecting groups. Chem.Res. Chin. Univ., **2016**, 32, 484-492.

(17) Wang, L., Hui, X., Geng, H. M., Ye, L., Zhang, A. Y., Shao, Z. Q. and Feng, Z.G.; Colloid

Polym. Sci.. **2017**, 295, 1549-1561.

(18) Hoshizawa, H., Minemura, Y., Yoshikawa, K., Suzuki, M. and Hanabusa, K; Thixotropic hydrogelators based on a cyclo(dipeptide) derivative. Langmuir, **2013**, 29, 14666-14673.

(19) Manchineella, S. and Govindaraju, T.; Molecular self-assembly of cyclic dipeptide derivatives and their applications. ChemPlusChem, **2017**, 82, 88-106.

(20) Makarevic, J., Jokic, M., Raza, Z., Stefanic, Z., Kojic-Prodic, B. and Zinic, M.; Chiral bis(amino alcohol)oxalamide gelators-gelation properties and supramolecular organization: racemate versus pure enantiomer gelation. Chemistry, **2003**, 9, 5567-5580.

(21) Dzolic, Z., Wolsperger, K. and Zinic, M.; Synergic effect in gelation by two-component mixture of chiral gelators. New J. Chem., **2006**, 30, 1411-1419.

(22) Parrish, D. A. and Mathias, L. J.; Five- and six-membered ring opening of pyroglutamic diketopiperazine. J. Org. Chem., **2002**, 67, 1820-1826.

(23) Merette, S. A. M., Burd, A. P. and Deadman, J. J.; ChemInform Abstract: Synthesis of 9-fluorenylmethyl esters using 9-fluorenylmethyl chloroformate. Tetrahedron Lett., **1999**, 40,753-754.

(24) Li, Y., Zhou, F., Wen, Y., Liu, K. Y., Chen, L. M., Mao, Y. Y., Yang, S. P. and Yi, T.; (-)-Menthol based thixotropic hydrogel and its application as a universal antibacterial carrier Soft Matter. **2014**, 10, 3077-3085.

(25) Ohsedo, Y., Oono, M., Saruhashi, K., Watanabe, H. and Miyamoto, N.; A new composite thixotropic hydrogel composed of a low-molecular-weight hydrogelator and a nanosheet. RSC Adv., **2014**, 4, 44837-44840.

(26) Nanda, J., Biswas, A. and Banerjee, A.; Single amino acid based thixotropic hydrogel formation and pH-dependent morphological change of gel nanofibers. Soft Matter, **2013**, 9, 4198-4208.

(27) Barbucci, R., Pasqui, D., Favaloro, R. and Panariello, G.; A thixotropic hydrogel from chemically cross-linked guar gum: synthesis, characterization and rheological behavior. Carbohydr. Res., **2008**, 18, 3058-3065.

(28) Jeong, B., Kim, S. W. and Baeabb, Y. H.; Thermosensitive sol-gel reversible hydrogels. Adv. Drug Deliver. Rev., **2002**, 54, 37-51.

(29) Latxague, L., Ramin, M. A., Appavoo, A., Berto, P., Maizani, M., Ehret, C., Chaszande, O. and Barthelemy, P.; Control of stem-cell behavior by fine tuning the supramolecular assemblies of low-molecular-weight gelators. Angew. Chem. Int. Ed., **2015**, 54, 4517-4521.

(30) Madhu, C., Voshavar, C., Rajasekhar K. and Govindaraju, T.; Cyclic dipeptide based cell-penetrating peptidomimetics for effective DNA delivery. Org. Biomol. Chem., **2017**, 15, 3170-3174.

(31) Loos, M. D., Feringa, B. L. and van Esch, J. H.; Design and application of self-assembled low molecular weight hydrogels. Eur. J. Org. Chem., **2005**, 3615-3631.

(32) Adams, D. J.; Dipeptide and tripeptide conjugates as low-molecular-weight hydrogelators. Macromol. Biosci., **2011**, 11, 160-173.

(33)Yuan, D. and Xu, B.; Heterotypic supramolecular hydrogels. J. Mater. Chem. B. **2016**, 4, 5638-5649.

(34) Shirakawa, M., Fujita, N. and Shinkai, S.; A stable single piece of unimolecularly pi-stacked porphyrin aggregate in a thixotropic low molecular weight gel: a one-dimensional molecular

template for polydiacetylene wiring up to several tens of micrometers in length. J. Am. Chem. Soc., **2005**, 127, 4164-4165.

(35) Liu, G. F., Zhang, D., Feng, C. L.; Progress of supramolecular chiral gel materials. Materials China. **2013**, 32, 420-430.

(36) Kar, T., Debnath, S., Das, D., Shome, A. and Das, P. K.; Organogelation and hydrogelation of low-molecular-weight amphiphilic dipeptides: pH responsiveness in phase-selective gelation and dye removal. Langmuir, **2009**, 15, 8639-8648.

(37) Hanabusa, K., Matsumoto, M., Kimura, M., Kakehi, A. and Shirai, H.; Low molecular weight gelators for organic fluids: gelation using a family of cyclo(dipeptide)s. J. Colloid Interf. Sci., **2000**, 224, 231-244.

(38) Suzuki, M., Yumoto, M., Shirai, H. and Hanabusa, K.; L-Lysine-based supramolecular hydrogels containing various inorganic ions. Org. Biomol. Chem., **2005**, 3, 3073-3078.

(39) Snyder, R. G.; Vibrational spectra of crystalline n-paraffins: Part I. Methylene rocking and wagging modes. J. Mol. Spectrosc., **1960**, 434,411-434.

(40) Cameron, D. G., Memura, J., Watrick, T. T. and Mantsch, H. H.; A fourier transform infrared study of the coagel to micelle transitions of sodium laurate and sodium oleate Colloids Surf., **1982**, 4, 131-145.

(41) Luo, X., Liu, B. and Liang, Y.; Self-assembled organogels formed by mono-chain L-alanine derivatives. Chem. Commun., **2001**, 17, 1556-1557.

(42) Huang, J. and Yu, L.; Effect of molecular chirality on racemate stability: α-Amino acids with nonpolar R groups. J. Am. Chem. Soc., **2006**, 128, 1873-1878.

(43) De Loos, M., van Esch, J. H. and Kellogg, R. M.; Angew. Chiral recognition in bis-urea-based aggregates and organogels through cooperative interactions. Chem. In. Ed.,

2001, 40,613-616.

(44) Dou, C., Wang, C., Zhang, H., Gao, H. and Wang, Y. Novel urea-functionalized quinacridone derivatives: ultrasound and thermo effects on supramolecular organogels. Chem. Eur. J., **2010**, 16, 10744-10751.